DOI. No. 10.13052/2794-7254.011

Spectral Sampling and Signal Decomposition (SSSD) for Improved Spectral Efficiency

Basim H. Mohammed and Seshadri Mohan*

Abstract: Spectrally Efficient Frequency Division Multiplexing (SEFDM) aims to enhance spectral efficiency by compressing subcarriers in the frequency domain, thereby reducing the required bandwidth. This approach primarily focuses on minimizing Inter-Carrier Interference (ICI), which typically necessitates a complex receiver design. We propose a simpler receiver design based on Spectral Sampling and Signal Decomposition (SSSD) technique. This technique facilitates the receiver to process Orthogonal Frequency Division Multiplexing (OFDM) signals outside the conventional orthogonality points in the frequency domain. Unlike traditional SEFDM approaches, the SSSD receiver utilizes interfering carriers as useful signals. Through simulations, we showcase the SSSD receiver's performance in extracting SEFDM signals and accommodating various pulse shapes beyond the conventional sinc pulse. However, our results also highlight a significant challenge posed by severely ill-conditioned matrices, which can be mitigated by exploring alternative pulse types.

Keywords: Faster-than-Nyquist, frequency division multiplexing, inter-carrier interference (ICI), orthogonal frequency division multiplexing (OFDM), spectral efficiency, spectrally efficient frequency division multiplexing (SEFDM).

1. Introduction

The electromagnetic spectrum is becoming an increasingly scarce resource due to the rise in wireless communication traffic and the inherent limitations of the available spectrum in supporting radio communication. Global mobile data traffic forecasts indicate that this upward trend in traffic volume will continue, with significant growth expected in the coming years [1, 2]. By 2029, mobile data traffic is projected to triple compared to 2023 levels [3]. Various approaches have been proposed in the literature to increase 5G network capacity, including techniques for improving Spectral Efficiency (SE) [4, 5], acquiring wider spectral capacity [6], applying intensive spectral reuse [7, 8], and the use of better resource sharing to achieve higher utilization [9, 10]. While each approach has contributed to increasing 5G network capacity, enhancements in SE at the waveform level have made the least contribution. These improvements in SE primarily stem from the integration of Multiple-Input Multiple-Output (MIMO) technology rather than the waveform itself. The increase in SE from 4G to 5G is lower than that achieved during the transition from 3G to 4G [11, 12].

The Spectrally Efficient Frequency Division Multiplexing (SEFDM) proposed in [13] offers an alternative waveform that enhances SE at the waveform level. By reducing subcarrier spacing and violating the orthogonality conditions, SEFDM extends Faster-than-Nyquist (FTN) scheme into the frequency domain [14]. Figure 1 illustrates and compares the concept of SEFDM with OFDM and FDM. As a non-orthogonal multicarrier technique, SEFDM reduces required bandwidth by allowing subcarrier overlapping and utilizing non-orthogonal waveforms. However, SEFDM inherits FTN's complexities, particularly in receiver design [15]. The first SEFDM scheme, fast-OFDM, aimed to double OFDM's data rate [13]. Subsequent research established a mathematical framework for SEFDM, employing complex receiver structures. Performance analysis of SEFDM using linear detectors and Genetic Algorithm (GA) detectors revealed lower Bit Error Rates (BER) compared to OFDM, but with increased iterations for additional subcarriers [16].

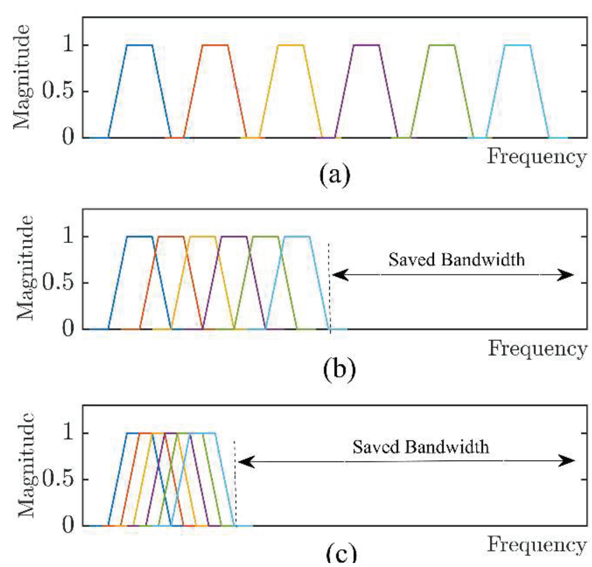

Figure 1.

Comparison of (a) FDM, (b) OFDM and (c) SEFDM in terms of savings in bandwidth.

Engineering and Information Technology School (EIT), University of Arkansas at Little Rock (UALR), Little Rock, AR 72204 USA
E-mail: bhmohammed@ualr.edu; sxmohan@ualr.edu
*Corresponding Author
Manuscript received 22 October 2024, accepted 25 October 2024, and ready for publication 21 December 2024.

Moreover, system performance degraded significantly with higher modulation orders. Simple linear detection methods (zero-forcing, MMSE, and TSVD) yielded minimal BER improvements [17]. On the other hand, applying the non-linear detection techniques such as iterative detection (ID) [18], sphere decoding (SD) [19], and fixed sphere decoding (FSD) [20] leads to increased receiver complexity with more subcarriers or higher modulation orders [18–20]. A two-stage decoder combining iterative detection and sphere decoding has also been explored [18,19]. Notably, the Bahl-Cocke-Jelinek-Raviv (BCJR) decoder achieved 40% bandwidth savings compared to OFDM, albeit with minor performance loss (less than 2 dB) and iterative processing in multipath fading channels [21]. Furthermore, SEFDM has been extended to radio-over-fiber systems [22].

Since its introduction over twenty years ago [13], the SEFDM approach to achieve higher spectral efficiency is based on mitigating the Inter-Carrier-Interference (ICI) effect resulting from the overlapping of compressed subcarriers that violate the orthogonality condition. To address ICI, SEFDM employs two primary strategies: (i) Utilizing complex decoders to minimize interference effects; (ii) Applying robust and heavy coding to extract symbols embedded in interference. These approaches view overlapping subcarriers as undesirable interference to be canceled, necessitating complex receiver designs. However, the Spectral Sampling and Signal Decomposition (SSSD) receiver introduced in [23] offers a promising alternative. Initially designed for OFDM, SSSD can detect symbols beyond orthogonality points, making it potentially suitable for extracting SEFDM signals. This paper explores modifying the SSSD receiver for SEFDM signal extraction, achieving higher spectral efficiency through reduced bandwidth requirements. Notably, the SSSD approach contrasts with SEFDM's ICI mitigation strategy, instead offering a straightforward and simple receiver structure.

2. The Spectral Sampling and Signal Decomposition (SSSD) Principle

The frequency domain representation of the OFDM signal $R(f)$ at the receiver can be modelled as:

$$R(f) = \frac{T}{2} \sum_{n=0}^{N-1} [X_n V(f - F_n) + X_n^* V(f + F_n)] \qquad (1)$$

for $-\infty < f < \infty$, where $X_n = |X_n| e^{-j\vartheta_n}$ is the transmitted symbol, $F_n = f_0 + \frac{n}{T}$, and $V(f)$ is the pulse shape in frequency domain, while T is the symbol duration, N is the number of subcarriers, and f_0 is the frequency of the first subcarrier. As shown in [23], Equation (1) can be simplified for the sampled received signal and written in matrix form as follow:

$$\mathbf{X} = 2\mathbf{R}\mathbf{V}^{-1} \qquad (2)$$

Where $\mathbf{R}$ is the FFT of the received signal evaluated at $f_k = \pm(f_0 + k/T + p(1/T))$ for $k = 0, 1, \ldots, N-1$ and the matrix $\mathbf{V}$ is found by evaluating;

$$V(f) = \left[\frac{sin\left(\frac{\pi L}{F_s} f\right)}{sin\left(\frac{\pi}{F_s} f\right)} \right] e^{-j\frac{\pi(L-1)}{F_s} f},$$

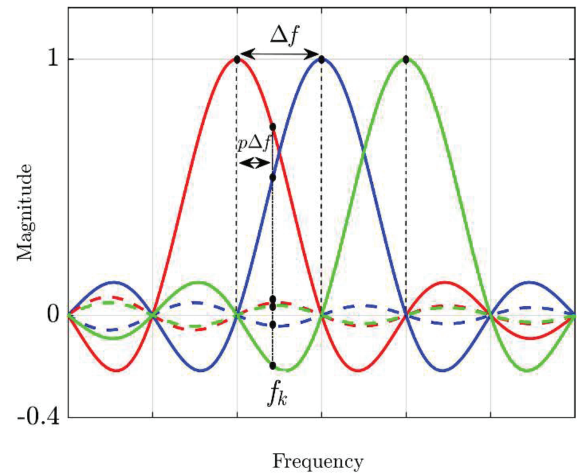

Figure 2.

The position of f_k in frequency domain and the role of p for an OFDM signal.

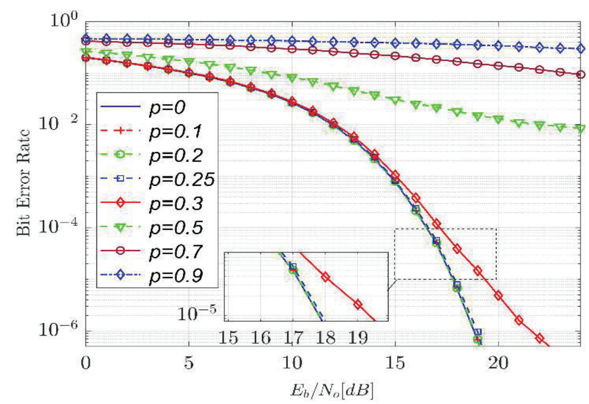

Figure 3.

BER Performance over AWGN channel with minimum number of 500 errors for each SNR value.

Table 1.

Simulation parameters	
Parameter	**Value**
Mapping	64-QAM
No. of subcarriers (N)	128
Subcarrier spacing (Δf)	15 kHz
Cyclic-Prefix length	16 samples
Delay spread for AWGN	1 sample

at $f = f_k$. p is a parameter used to specify the spectral sampling point deviation from orthogonality points and it can take any value in the range $-1 < p < 1$ as shown in Figure 2. In other words, the spectral sampling points will experience a deviation of $p(1/T)$ Hz from the orthogonality points. The simulation results for the AWGN channel for $p = 0, 0.1, 0.2 \ldots 0.9$, shown in Figure 3 using the parameters listed in Table 1. It can be seen that SSSD can detect the OFDM symbols beyond the orthogonality point and

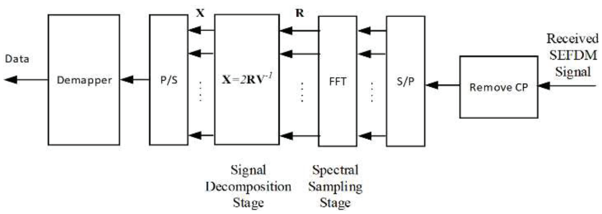

Figure 4.
The SSSD receiver for SEFDM signal.

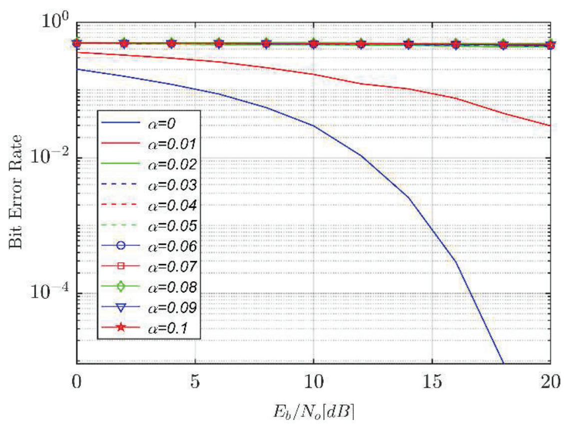

Figure 5.
BER performance using different values of α with minimum of 300 errors for each SNR value.

deliver the same performance for $p < 0.25$ and the performance degraded rapidly for $p < 0.25$. Since the SSSD has the capability to detect the OFDM signal in the presence of ICI, then the next logical step is to use it in receiving the SEFDM signal.

3. SSSD Receiver Performance for SEFDM Signal

The SSSD can be adopted to receive and extract the symbols carried by the SEFDM signal. The SEFDM signal is similar to the OFDM signal with the exception that the subcarriers frequency spacing (Δf) is less than the OFDM symbol rate; $\Delta f < \frac{1}{T}$, which produce non-orthogonal signal. While f_k is defined for all values of k to be: $f_k = f_0 + (1 - \alpha)\frac{1}{T}$, where α is defined to be the compression ratio. By modifying the **V** matrix according to the desired α value, then, the SSSD receiver can be used to receive the SEFDM signal. Figure 4 depict the SSSD receiver for SEFDM signal. Figure 5 illustrates the BER performance of SEFDM signals utilizing the SSSD receiver for various values of α. Figure 6 show the impact of α on the noise power level per subcarrier, revealing that the noise coloration effect of α accompanied by a substantial increase in the noise level even with a minor increment in α. The simulation parameters shown in Table 2.

4. Using Raised Cosine and Triangular Pulses

The utilization of a rectangular pulse in OFDM and SEFDM yields a *sinc*-shaped subcarrier spectrum, which is sampled to construct

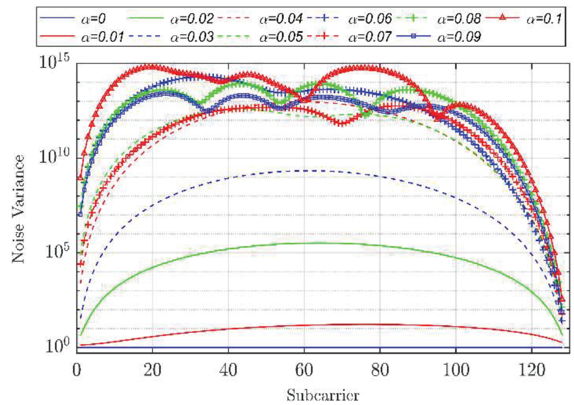

Figure 6.
Noise Power distribution per subcarrier for different values of α.

Table 2.

Simulation parameters for SEFDM	
Parameter	**Value**
Mapping	64-QAM
No. of subcarriers (N)	128
Subcarrier spacing (Δf)	15 kHz
Compression ratio (α)	0, 0.01, 0.02,...0.09, 0.1
Cyclic-Prefix length	16 samples
Delay spread for AWGN	1 sample

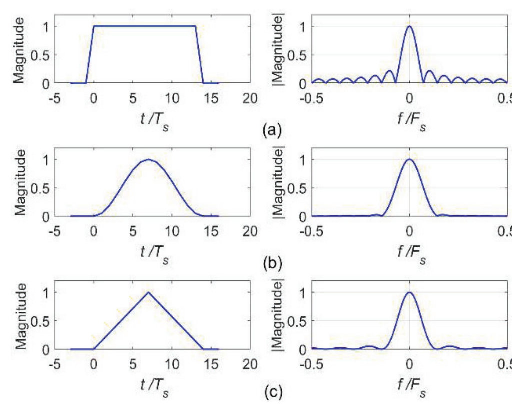

Figure 7.
The spectrum of (a) Rectangular (b) Raised Cosine and (c) Triangular pulse.

the **V** matrix. The chosen pulse shape significantly influences the properties of the **V** matrix. To enhance the system performance, alternative pulses with diverse spectral characteristics can be explored to modify the **V** matrix.

For the purpose of comparison, two pulses are selected with *sinc* or *sinc*-like spectrum: the Raised Cosine (RC) with a roll-off factor of one and the triangular pulse. Notably, both exhibit a distinctive main lobe in their spectra as displayed in Figure 7. The DTFT expressions for the RC and triangular pulses, respectively, for a symbol period of T, are:

$$V_{RC}(f) = \frac{1}{2L}\left[\frac{sin\left(\frac{\pi L}{F_s}f\right)}{sin\left(\frac{\pi}{F_s}f\right)}\right]e^{-j\frac{\pi(L-1)}{F_s}f} - \frac{1}{4L}\left[\frac{sin\left(\frac{\pi L}{F_s}\left(f-\frac{1}{T}\right)\right)}{sin\left(\frac{\pi}{F_s}\left(f-\frac{1}{T}\right)\right)}\right]e^{-j\frac{\pi(L-1)}{F_s}\left(f-\frac{1}{T}\right)} - \frac{1}{4L}\left[\frac{sin\left(\frac{\pi L}{F_s}\left(f+\frac{1}{T}\right)\right)}{sin\left(\frac{\pi}{F_s}\left(f+\frac{1}{T}\right)\right)}\right]e^{-j\frac{\pi(L-1)}{F_s}\left(f+\frac{1}{T}\right)} \quad (3)$$

$$V_{TRI}(f) = \frac{1}{2}\left[\frac{2}{L}\frac{sin\left(\frac{\pi L}{2F_s}f\right)}{sin\left(\frac{\pi}{F_s}f\right)}e^{-j\frac{\pi L}{2F_s}f}\right]^2 \quad (4)$$

Figures 8 and 9, respectively, depict the effect of α on the noise power level using RC and triangular pulses. Similarly, Figures 10 and 11, respectively, illustrate the BER performance of SEFDM receiver for various values of α using RC and triangular pulses. Additionally, Figure 12 compares the condition number of the **V** matrix for the rectangular, RC, and triangular pulses, revealing a significant increase as α increases. The results demonstrate

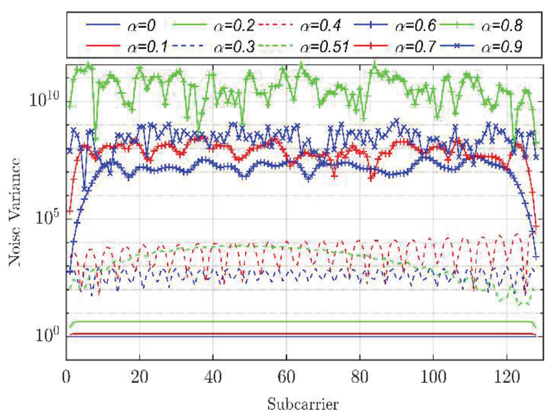

Figure 8.

Noise power distribution per subcarrier for the RC pulse using different values of α.

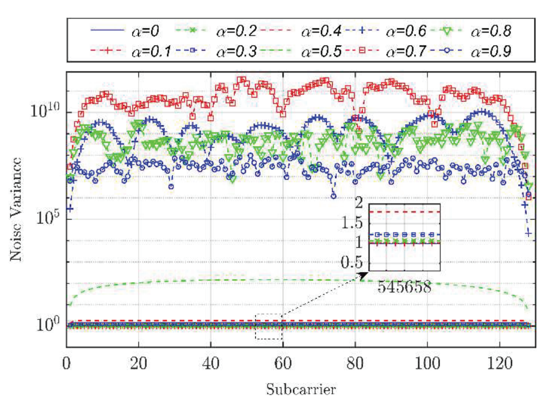

Figure 9.

Noise Power distribution per subcarrier for the triangular pulse using different values of α.

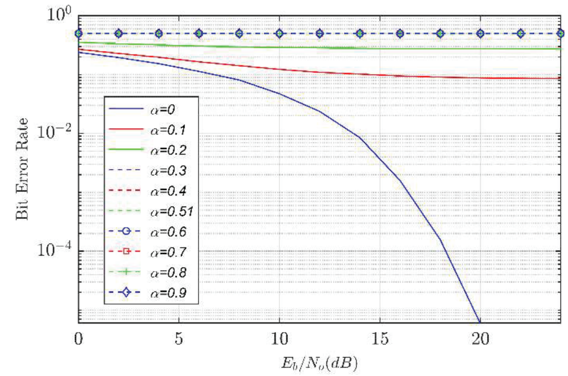

Figure 10.

BER Performance for RC pulse with minimum of 500 errors for each SNR value.

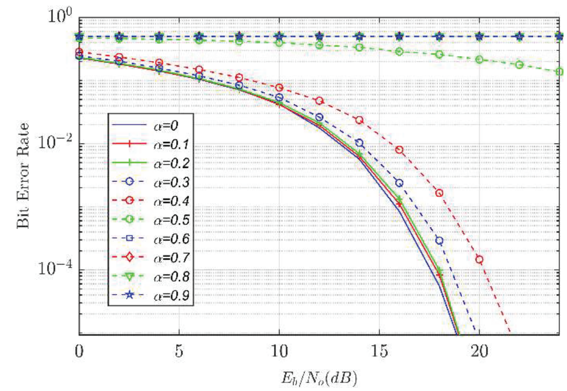

Figure 11.

BER Performance triangular pulse with minimum of 500 errors for each SNR value.

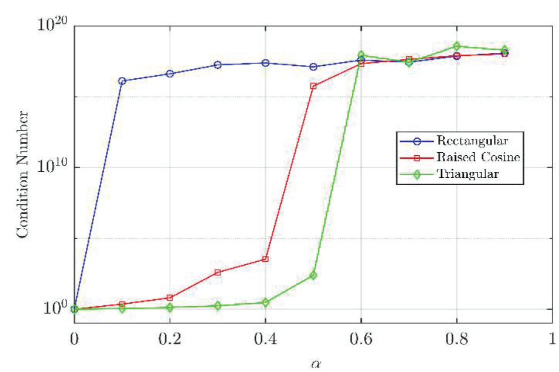

Figure 12.

The **V** matrix condition number comparison for the rectangular, RC and triangular pulses.

that increasing α severely ill-conditions the **V** matrix, leading to substantial increase in noise levels and performance degradation. The simulation parameters employed are identical to those summarized in Table 2, except the subcarrier spacing (Δf) is doubled to maintain orthogonality condition for the RC and Triangular pulses.

5. Simulation Results Discussion

The SSSD receiver's performance deteriorates rapidly as subcarriers are compressed in the frequency domain for non-zero values of α. Even a small α value of 0.01 causes the **V** matrix to become ill-conditioned, significantly increasing noise levels (Figures 5 and 6). Since the **V** matrix is derived from the spectral samples of the applied pulse, modifying the pulse shape alters the matrix properties. To compare performance, RC and Triangular pulses are evaluated alongside the conventional rectangular pulse.

Assuming preserved orthogonality at $\alpha = 0$, the SSSD receiver is tested with these pulses, requiring twice the frequency spacing used for the sinc pulse. Results show that the pure RC pulse yields relatively lower noise levels than the sinc pulse, though still high, leading to degraded performance due to the ill-conditioned **V** matrix (Figures 5 and 6). Notably, for the RC pulse, $\alpha = 0.51$ is used, as the **V** matrix becomes singular and non-invertible at $\alpha = 0.5$.

Figure 12 compares the condition numbers of the **V** matrix for three pulse shapes, revealing the Triangular pulse yields a better-conditioned matrix for $\alpha < 0.5$. This corresponds to lower noise levels and improved performance, as shown in Figures 9 and 11. Specifically, the SSSD receiver achieves near-orthogonal performance using the Triangular pulse for $\alpha < 0.2$, with gradual degradation beyond this threshold. The Triangular pulse offers enhanced performance relative to the RC pulse for $\alpha < 0.4$. The **V** matrix's condition significantly impacts noise levels, as its ill-conditioning amplifies noise power experienced by each subcarrier. Despite using different pulses, OFDM maintains better SE than the SSSD receiver for SEFDM signals, primarily due to OFDM's ability to maintain orthogonality at lower subcarrier frequency spacing.

6. Conclusion

The SSSD receiver can extract non-orthogonal SEFDM signals for various compression ratios, provided the **V** matrix is well-conditioned. However, as matrix condition deteriorates, noise level increases. Thus, the primary obstacle lies in the **V** matrix's condition, rather than inter-carrier interference (ICI). This study introduces a new perspective on the SEFDM problem, reframing it as an ill-conditioned matrix problem. Two approaches can be employed to address this: (i) Engineering approach: By designing pulses yielding well-conditioned matrices, and (ii) Mathematical approach: By modifying the matrix conditions.

To enhance SEFDM signal detection accuracy using SSSD receivers, we propose four research directions: (1) Pulse design: Create pulses yielding well-conditioned **V** matrices, (2) Diverse pulse sets: Employ varied pulses across subcarriers, (3) Non-uniform spacing and sampling: Explore non-uniform subcarrier spacing and spectral sampling, and (4) Matrix regularization: Utilize regularization or decomposition methods for invertible matrices with minimal error.

References

[1] E. Selvamanju and V. B. Shalini, "Archimedes Optimization Algorithm with Deep Belief Network Based Mobile Network Traffic Prediction for 5G Cellular Networks," in *2022 4th International Conference on Smart Systems and Inventive Technology (ICSSIT)*, Jan. 2022, pp. 370–376. doi:10.1109/ICSSIT53264.2022.9716552.

[2] S. Smys, J. I. Z. Chen, and S. Shakya, "Survey on neural network architectures with deep learning," *Journal of Soft Computing Paradigm (JSCP)*, vol. 2, no. 03, pp. 186–194, 2020.

[3] Ericsson, "Ericsson Mobility Report," Stockholm, Sweden, Nov. 2023. Accessed: Mar. 30, 2024. [Online]. Available: https://www.ericsson.com/en/reports-and-papers/mobility-report/reports/november-2023.

[4] J. G. Andrews et al., "What Will 5G Be?," *IEEE Journal on Selected Areas in Communications*, vol. 32, no. 6, pp. 1065–1082, Jun. 2014, doi:10.1109/JSAC.2014.2328098.

[5] F. Boccardi, R. Heath, A. Lozano, T. L. Marzetta, and P. Popovski, "Five disruptive technology directions for 5G," *IEEE Communications Magazine*, vol. 52, no. 2, pp. 74–80, 2014.

[6] M. J. Marcus, "ITU WRC-19 Spectrum Policy Results," *IEEE Wireless Communications*, vol. 26, no. 6, pp. 4–5, Dec. 2019, doi:10.1109/MWC.2019.8938175.

[7] Y. Yang, B. Bai, and W. Chen, "Spectrum Reuse Ratio in 5G Cellular Networks: A Matrix Graph Approach," *IEEE Transactions on Mobile Computing*, vol. 16, no. 12, pp. 3541–3553, Dec. 2017, doi:10.1109/TMC.2017.2696005.

[8] D. Verenzuela and G. Miao, "Scalable D2D Communications for Frequency Reuse ≫1 in 5G," *IEEE Transactions on Wireless Communications*, vol. 16, no. 6, pp. 3435–3447, Jun. 2017, doi:10.1109/TWC.2017.2679001.

[9] M. K. Singh, S. Vittal, and A. Antony Franklin, "SERENS: Self Regulating Network Slicing in 5G for Efficient Resource Utilization," in *2020 IEEE 3rd 5G World Forum (5GWF)*, Sep. 2020, pp. 590–595. doi:10.1109/5GWF49715.2020.9221405.

[10] H.-H. Chang, L. Liu, and Y. Yi, "Deep Echo State Q-Network (DEQN) and Its Application in Dynamic Spectrum Sharing for 5G and Beyond," *IEEE Transactions on Neural Networks and Learning Systems*, vol. 33, no. 3, pp. 929–939, Mar. 2022, doi:10.1109/TNNLS.2020.3029711.

[11] GSMA, "The 5G Guide a Reference for Operators," Apr. 2019. Accessed: Jul. 30, 2020. [Online]. Available: https://www.gsma.com/wp-content/uploads/2019/04/The-5G-Guide_GSMA_2019_04_29_compressed.pdf.

[12] M. Ramesh, C. G. Priya, and V. P. M. B. A. A. Ananthakirupa, "Design of efficient massive MIMO for 5G systems – Present and past: A review," in *2017 International Conference on Intelligent Computing and Control (I2C2)*, Jun. 2017, pp. 1–4. doi:10.1109/I2C2.2017.8321950.

[13] M. R. Rodrigues and I. Darwazeh, "Fast OFDM: A proposal for doubling the data rate of OFDM schemes," *Proceeding of the International Conference on Telecommunications*, pp. 484–487, Jun. 2002.

[14] J. B. Anderson, "Faster-than-Nyquist Signaling for 5G Communication," in *Signal Processing for 5G: Algorithms and Implementations*, F. Luo and C. Zhang, Eds., Wiley-IEEE Press, 2016, pp. 24–46.

[15] I. Darwazeh, T. Xu, and R. C. Grammenos, "Bandwidth-compressed multicarrier communication: SEFDM," in *Signal Processing for 5G: Algorithms and Implementations*, F. Luo and C. Zhang, Eds., Wiley-IEEE Press, 2017, pp. 90–114.

[16] M. R. D. Rodrigues and I. Darwazeh, "A Spectrally Efficient Frequency Division Multiplexing Based Communication System," in

Proceedings of the 8th International OFDM-Workshop (InOWo'03), no, 2003, pp. 70–74,.

[17] S. Isam, I. Kanaras, and I. Darwazeh, "A Truncated SVD approach for fixed complexity spectrally efficient FDM receivers," in *2011 IEEE Wireless Communications and Networking Conference, WCNC 2011*, 2011.

[18] T. Xu, R. C. Grammenos, F. Marvasti, and I. Darwazeh, "An improved fixed sphere decoder employing soft decision for the detection of non-orthogonal signals," *IEEE Communications Letters*, vol. 17, no. 10, pp. 1964–1967, 2013.

[19] I. Kanaras, A. Chorti, M. R. Rodrigues, and I. Darwazeh, "A fast constrained sphere decoder for ill conditioned communication systems," *IEEE Communications Letters*, vol. 14, no. 11, pp. 999–1001, 2010.

[20] S. Isam and I. Darwazeh, "Design and performance assessment of fixed complexity spectrally efficient FDM receivers," in *IEEE Vehicular Technology Conference*, 2011.

[21] T. Xu and I. Darwazeh, "A soft detector for spectrally efficient systems with non-orthogonal overlapped sub-carriers," *IEEE Communications Letters*, vol. 18, no. 10, pp. 1847–1850, 2014.

[22] S. Mikroulis, T. Xu, J. E. Mitchell, and I. Darwazeh, "First demonstration of a spectrally efficient FDM radio over fiber system topology for beyond 4G cellular networking," in *2015 20th European Conference on Networks and Optical Communications, NOC 2015*, 2015.

[23] B. H. Mohammed and S. Mohan, "Highly Immune-Orthogonal Frequency Division Multiplexing (HI-OFDM)," *Submitted to IEEE Access*, Aug. 2024.

Biographies

Basim H. Mohammed received BS degree in Electronics and Communications Engineering (1998) and an MS degree in Communications Engineering (2001) from Al-Nahrain University, Iraq. Worked as a lab instructor at Al-Nahrain University before joining the industry. He has over a decade of industry experience working with leading telecommunications companies, including Motorola, NSN (Nokia-Siemens Networks), and Huawei Technologies. His expertise spans RF optimization and cellular network planning, with notable contributions to the RF optimization and KPI enhancement of 2G and 3G cellular networks in Iraq. His research interests lie at the intersection of signal processing, multicarrier communication systems, and artificial intelligence. Currently, he is a Ph.D. student in Engineering Sciences and Systems/Telecommunications Track at the University of Arkansas at Little Rock (UALR), AR, USA.

Seshadri Mohan [IEEE Life Senior Member] is currently a professor in the Systems Engineering Department at the University of Arkansas at Little Rock, where, from August 2004 to June 2013, he served as the chair of the Department of Systems Engineering. Prior to his current position he served as the CTO of Comverse. Besides these positions, his industry experience spans Telcordia (formerly Bellcore), Bell Laboratories, and Clarkson and Wayne State Universities. He has authored/coauthored over 140 publications as books, patents, and papers in refereed journals and conference proceedings. He co-authored the textbook Source and Channel Coding: An Algorithmic Approach. He holds 14 patents. He received the 2010 IEEE Region 5 Outstanding Engineering Educator Award. He holds a Ph.D. degree in electrical and computer engineering from McMaster University, Canada, a Master's degree in electrical engineering from the Indian Institute of Technology, Kanpur, and a Bachelor's degree in electronics and telecommunications from the University of Madras, India.